Cell. Mol. Biol. (ISSN: 1165-158X)

Journal Homepage: www.cellmolbiol.org

Cellular and Molecular Biology

Original Article

Folic acid-decorated tamoxifen-loaded covalent organic framework induces apoptosis in MCF-7 breast cancer cells via BAX/Caspase-8 upregulation

Akash Chandran[1,3], Sudhina S.[1,2], Radhika A.[4], Muthunayagam Vibin[5], Janeesh Plakkal Ayyappan[1,2,3*]

[1] *Centre for Advanced Cancer Research, Department of Biochemistry, University of Kerala, Kariavattom Campus, Thiruvananthapuram-695034, Kerala, India*
[2] *Translational Nanomedicine and Life Style Disease Research Laboratory, Department of Biochemistry, University of Kerala, Kariavattom Campus, Thiruvananthapuram- 695581, Kerala, India*
[3] *Department of Nanoscience and Nanotechnology, University of Kerala, Kariavattom Campus, Thiruvananthapuram- 695581, Kerala, India*
[4] *Department of Biochemistry, Government Arts and Science College, Kulathoor, Neyyattinkara-695506, Thiruvananthapuram, India*
[5] *Department of Biochemistry, St. Albert's College (Autonomous), Mahatma Gandhi University, Ernakulam-682018, India*

Article Info

Article history:

Received: July 08, 2025
Accepted: October 29, 2025
Published: January 31, 2026

Use your device to scan and read the article online

Abstract

The side effects and non-specific targeting of healthy organs associated with conventional cancer therapies necessitate the design and fabrication of novel nanomaterial-based drug delivery systems. In this study, we successfully fabricated a novel two-dimensional (2D) covalent organic framework (COF) nanomaterial. This COF was loaded with tamoxifen (TMX) and surface-modified with folic acid (FA) to achieve effective targeting for breast cancer therapy. The resulting construct, TMX@COF-FA, was characterized using PXRD, FTIR, ^{13}C NMR, CHNS analysis, BET surface area analysis, TGA, UV-Vis spectroscopy, SEM, and EDX analysis. The COF carrier demonstrated a high drug encapsulation efficiency of approximately 82%. Furthermore, it exhibited a pH-responsive drug release profile, with a significantly higher release rate at pH 5.4 compared to pH 7.4, which is ideal for the acidic tumor microenvironment. Cell viability studies revealed that TMX@COF-FA induced about 90% cell death in MCF-7 breast cancer cells, while showing minimal cytotoxicity in L929 fibroblast cells. The mechanism of cell death was investigated using AO/EtBr dual staining, ROS detection assays, flow cytometry (FACS), and qRT-PCR. Collectively, our findings demonstrate that the FA-conjugated COF can efficiently deliver TMX to MCF-7 cells via folate receptor-mediated endocytosis, leading to potent cancer cell destruction. This study underscores the potential of functionalized COFs as promising targeted drug delivery platforms for breast cancer treatment.

Keywords: Covalent Organic Frameworks, Tamoxifen, Folic Acid, MCF-7, Targeted drug delivery.

1. Introduction

In step with the demands of modern life, cancer stands as a predominant lifestyle disease, responsible for high mortality and poor survival rates in women globally. Breast cancer is one of the common heterogeneous diseases occurring in females, which accounts for 30% of all malignancies faced by females[1-3]. In breast cancer cells, the estrogen receptors (ER^+) are positive, which shows a marker for breast cancer [3]. Even though there are several conventional treatment therapies, such as chemotherapy, immunotherapy and surgery [4-6], which lack efficiency in curing this disease and cause several side effects, such as adverse effects on bone marrow suppression, hair loss, gastrointestinal reaction[7,8]. Therefore, to overcome these lacunas of conventional therapies, it is necessary to develop advanced therapeutic devices for targeted and efficient drug delivery. In the past two decades, nanomaterial-based therapies have emerged to increase the therapeutic efficiency. Initially, metal nanoparticles such as gold and silver nanoparticles were synthesized via different approaches for therapeutic applications. However, metal nanoparticles often face significant limitations that hinder their clinical translation. A primary concern is their potential toxicity, which, although sometimes mild, raises safety issues [9, 10]. Furthermore, many metal nanoparticles exhibit low renal clearance, leading to prolonged circulation and increased risk of long-term side effects [11, 12]. This, coupled with their non-specific biodistribution and untargeted accumulation in healthy organs (e.g., liver and spleen), can result in off-target effects [13, 14]. These combined drawbacks limit the potential of many metal nanoparticles for safe and effective biomedical applications, both *in vitro* and *in vivo*.

To mitigate these drawbacks, scientists focused on

* Corresponding author.
E-mail address: janeeshbiochemistry@keralauniversity.ac.in (Janeesh P.A.).
Doi: http://dx.doi.org/10.14715/cmb/2025.72.1.4

developing robust, potential, biocompatible and non-toxic nano-carriers for efficient and targeted delivery of anti-cancer therapeutic agents. The administration of pharmaceuticals into the cells via targeted nano-carriers will be an alternative and efficient method for the treatment of cancer. For this, a new class of porous crystalline metal-free nano material, namely covalent organic frameworks (COFs), has emerged and attracted scientists who work in the arena of cancer therapy. [15–20].

Covalent organic frameworks are crystalline, extended two-dimensional (2D) and three-dimensional (3D) structures formed by joining molecular building units with strong covalent bonds aroused more attention in catalysis,[21,22] sensing,[23,24] separation,[25] adsorption, gas storage energy, biomedicine,[26,27] and drug delivery[28] due to their intrinsic properties such as tuneable and permanent porosity[29,30–32], high surface area[33], low density[34] and high thermal stability[35]. Moreover, rather than these intrinsic properties, the ease of handling, synthesis procedures and pre-designable structures make them a potential candidate for wide range of applications [21,36,37].

Unlike other porous polymeric materials, COFs are formed by reversible condensation of secondary building groups, which enables them to retain their crystallinity and biodegradability. Additionally, the absence of metals in COFs prevents potential biological toxicity[38], which offers ample scope in biomedical applications, especially in targeted drug delivery. The main feature of COF is that the high surface area and tunable porosity, which enables COFs to internalize therapeutic agents into their framework structure and the surface active sites enable ease of functionalization and thereby enable a new platform for targeted therapeutic applications [28,29,33]. Even though COFs are an excellent candidate for various applications, their biomedical explorations are still in infant stage and COF-assisted drug delivery began in 2016 [39].

Adjuvant endocrine treatment with tamoxifen is most well-known to date. Tamoxifen has been demonstrated to be an effective antagonist, lowering both the death and recurrence rates in ER^{+ve} breast cancer patients by about 30% and 40%, respectively [40,41]. Although tamoxifen is an effective and affordable first-line treatment for breast cancer, its clinical utility is constrained by significant challenges. These include dose-limiting systemic side effects and the need to reduce the required therapeutic dosage to minimize toxicity. To address these limitations, the development of advanced nano-formulations for the efficient and targeted delivery of therapeutics is imperative.

Folic acid receptor (FR), a 38 kDa glycosylphosphatidylinositol (GPI)-anchored protein, is overexpressed in a variety of tumour cells, including lung, ovarian, brain, head-neck, and breast malignancies, while modest amounts are observed in healthy cells. Folic acid (FA) is a bioactive molecule frequently employed to functionalize drug delivery systems in cancer therapy. It is an anionic molecule that does not diffuse readily through cellular membranes. Folic acid (FA) satisfies the effective targeting by binding to the folate receptors that are overexpressed on the surface of cancer cells [42,43].

Despite the benefits of currently available anticancer drugs, such as tamoxifen (TMX), their goal is restricted because of their poor tumour tissue penetration, undesirable side effects, and slow evolution of tumour cell resistance. So, the primary objective of this study is to increase the targeted uptake and decrease the off-target toxicity of drugs used to treat breast cancer. To this end, we designed and fabricated a novel two-dimensional (2D) crystalline porous covalent organic framework (COF) via a solvothermal method. The framework was synthesized through the condensation of 2,6-pyridinedicarboxylic acid and 4,4'-diaminodiphenylmethane, forming robust amide linkages [43]. Subsequently, the synthesized COF was loaded with tamoxifen as a model chemotherapeutic agent. The tamoxifen-loaded COF (TMX@COF) was then functionalized with the folate receptor-targeting ligand, folic acid (FA), to enhance its cellular uptake via receptor-mediated endocytosis in cancer cells. Subsequently, we evaluated and compared the cytotoxicity of the targeted (TMX@COF-FA) and non-targeted (TMX@COF) formulations against both MCF-7 human breast cancer cells and L929 fibroblast cells. The pH-responsive drug release profile of the targeted formulation (TMX@COF-FA) was also assessed under simulated physiological (pH 7.4) and pathological (pH 5.4) conditions. Finally, the comparative anti-cancer efficacy of the targeted versus non-targeted systems was investigated through a series of assays, including acridine orange/ethidium bromide (AO/EtBr) dual staining, reactive oxygen species (ROS) detection, wound healing, quantitative reverse transcription polymerase chain reaction (qRT-PCR), and flow cytometry analysis.

2. Materials and Methods

2.1. Materials used

All the chemicals were purchased and used without any purification. Thionyl chloride ($SOCl_2$) (sigma Aldrich), 2, 6-pyridinedicarboxilic acid (sigma Aldrich), Dichloro Methane (DCM) (sigma Aldrich), 4, 4'-diaminodiphenyl methane (DDM) (sigma Aldrich), Ammonium chloride (NH_4Cl) and Sodium sulphate (Na_2SO_4), Tamoxifen Citrate (sigma Aldrich), phosphate buffered saline (pH=7.4 & 5.4), Fetal Bovine Serum (FBS), Dulbecco's Modified Eagle Medium (DMEM), trypsin, pen-strep antibiotics, 3-(4,5-dimethylthiazol-2-yl)-2,5-diphenyl-2H- tetrazolium bromide (MTT), dimethyl sulfoxide (DMSO), ethanol, deionized water and MCF-7 human breast cancer cells and L929 Fibroblast cells.

2.3. Methods

2.3.1. Preparation of 2D COF

2,6-Pyridinedicarboxylic acid (0.05 g, 3.0 mmol) was suspended in thionyl chloride (4.0 mL). The mixture was refluxed under an argon atmosphere for 16 hours, yielding a clear yellow solution. Excess thionyl chloride was removed under reduced pressure. The resulting acid chloride residue was dissolved in anhydrous dichloromethane (10 mL) and cooled to 0 °C in an ice bath. A solution of 4,4'-diaminodiphenylmethane (DDM) in anhydrous dichloromethane (2.5 mL) was added dropwise via cannula. The reaction mixture was stirred at room temperature for 16 hours, during which a pale yellow precipitate formed. The precipitate was collected by filtration and washed with a half-saturated aqueous ammonium chloride solution (2 × 3 mL). The organic phase was dried over anhydrous sodium sulfate, filtered, and concentrated under reduced pressure. The resulting solid was dried under vacuum to afford the COF as a pale yellow powder [45].

2.3.2. Modification of drug delivery system with folic acid

The coupling of folic acid at the surface of the drug delivery system was achieved by using the method in previous reports [46]. Briefly, the folic acid was activated by adding 10 mg of EDC and 6 mg of NHS. Afterward, the activated folic acid was added dropwise to the dispersion containing tamoxifen loaded drug delivery system in double-distilled water. Then this mixture was vortexed and incubated for 3 hours, filtered and dried.

2.3.3. Drug loading to the delivery system

Drug loading was performed via a solution immersion method. Briefly, a solvent-free COF sample (200 mg) was immersed in 10 mL of a 0.1 M tamoxifen solution in ethanol. The mixture was stirred for 12 hours at room temperature, with the container sealed to prevent solvent evaporation. Subsequently, the solvent was removed under reduced pressure. The resulting tamoxifen-loaded COF (TMX@COF) was dried in a hot air oven, thoroughly washed with ethanol (multiple times) followed by deionized water to remove any surface-adsorbed drug, and finally dried at room temperature prior to use [47,48]. The drug loading efficiency (DLE) and encapsulation efficiency (EE) were calculated by the equation;

$$\text{Drug Loading Efficiency (DLE)} = \frac{\text{Weight of Drug in Nanocarrier}}{\text{Weight of Nanocarrier}} \times 100$$

2.3.4. In vitro drug release study

Drug release profile was done in both acidic pH (5.4) and physiological conditions (pH=7.4). In brief, 100 mg of site-targeted drug-loaded COF (TMX@COF-FA) is dispersed in 10 mL of simulated body fluid (SBF) of pH 7.4 and 5.4 and stirred at 37 °C. At predetermined time intervals (0, 1, 6, 12, 24 & 48 hours), 3 mL of dissolution medium was collected and replaced with fresh SBF [49,47]. The collected medium was subjected to UV-Vis spectrophotometry to determine the drug concentration.

2.3.5. Cytotoxicity assay by MTT

MCF-7 human breast cancer cells were obtained from the National Centre for Cell Science (NCCS, Pune, India). The cells were maintained in Dulbecco's Modified Eagle Medium (DMEM) supplemented with 10% fetal bovine serum (FBS) and 1% penicillin-streptomycin (100 U/mL) at 37 °C in a humidified atmosphere containing 5% CO_2.

For the cell viability assay, an MTT kit (Himedia) was used according to the manufacturer's instructions. Briefly, cells were seeded in a 96-well plate at a density of 5 × 10^3 cells per well and allowed to adhere for 24 hours. Subsequently, the cells were treated with various concentrations (10, 15, 20, 25, and 30 µg/mL) of the following formulations: the pristine COF, free tamoxifen (TMX), the non-targeted drug-loaded COF (TMX@COF), and the folic acid-conjugated targeted formulation (TMX@COF-FA). After 24 hours of incubation, the medium was replaced with fresh medium containing 10 µL of MTT reagent per well, followed by incubation for 4 hours at 37 °C in the dark. The resulting formazan crystals were dissolved by adding 100 µL of dimethyl sulfoxide (DMSO) to each well. Finally, the absorbance of each well was measured at 570 nm using a microplate reader. [50]. The percentage of viability was calculated using the equation,

$$\text{Percentage of cell viability} = \frac{\text{The Absorbance of Test}}{\text{The Absorbance of Control}} \times 100$$

2.3.6. Acrydine orange & ethidium bromide dual staining assay

The MCF-7 (human breast cancer) cells were cultured in a 96-well plate in a 5% CO_2 atmosphere at 37 °C. After 24 hours of incubation, the cells were treated with COF (50 µg mL^{-1}), TMX (50 µg mL^{-1}) and COF-TMX (50 µg mL^{-1}). After incubation for 24 hours, a mixture of dyes containing equal volume (100 µg/mL) of acridine orange (AO) and ethidium bromide (EtBr) was added and after 10 minutes of incubation, the treated cells were washed twice with PBS and visualized under a fluorescence microscope[50].

2.3.7. ROS staining assay

The generation of intracellular ROS was evaluated by DCFH-DA. MCF-7 (human breast cancer) cells were seeded in 96-well plates at a density of 1 × 10^4 cells per well for 24 hr. Then the cells were treated with COF (50 µg mL^{-1}), TMX (50 µg mL^{-1}), TMX@COF (50 µg mL^{-1}) and TMX@COF-FA (50 µg mL^{-1}) for 24 h at 37 °C. After incubation, the cells were loaded with DCFH-DA (10 µM) for 20 min and washed three times with PBS to remove the free DCFH-DA[51]. The fluorescence images of the cells were acquired using a fluorescent microscope with excitation wavelength at 488 nm and emission wavelength from 525 nm. The cells were trypsinized and suspended in PBS and fluorescent generation was quantified by flow cytometry.

2.3.8. Gene expression by qRT-PCR analysis

To elucidate the apoptotic mechanism, quantitative real-time PCR (qRT-PCR) was performed. MCF-7 cells were seeded in 6-well plates at a density of 5 × 10^4 cells per well. Upon reaching approximately 80% confluence, the cells were treated for 24 hours with 50 µg mL^{-1} of the following: the pristine COF, free tamoxifen (TMX), the non-targeted TMX@COF, and the targeted TMX@COF-FA formulation. Following treatment, total RNA was isolated from the cells using TRIzol™ reagent (Origin, India) and purified with the Thermo Scientific GeneJET RNA Purification Kit according to the manufacturer's instructions. Subsequently, cDNA was synthesized from 1 µg of total RNA using the Verso cDNA Synthesis Kit (Thermo Fisher Scientific, USA). Quantitative PCR was carried out on a Bio-Rad real-time PCR system using 100 ng of cDNA template per reaction and the SYBR Green qPCR Master Mix (Thermo Fisher Scientific, USA). [52]. Data were normalized to a housekeeping gene GAPDH. Primer sequences are listed in Table S1.

2.3.9. Wound healing assay

The effect of the formulations on cell proliferation was studied in confluent monolayers of MCF-7 human breast cancer cells by scratch wound assay. In brief, MCF-7 cells were cultured in a 6-well plate and after 80% confluence, the cell layers were scraped using a sterile tip to form the wound. After wound formation, the detached cells were discarded by washing with PBS. Then the scratched cells were exposed to 50 µg/mL of COF, TMX, TMX@COF, TMX@COF-FA and cells without any formulations (control) for 24 hours in 5% CO_2 at 37 °C. At 6-hour intervals, the images were taken using confocal microscope [53].

2.3.10. Statistical analysis

Results are expressed as average ±SD of three independent experiments and analysed by one-way analysis of variance using GraphPad Prism software and the differences were considered statistically significant at $p \leq 0.05$ (*), $p \leq 0.01$ (**) and $p \leq 0.001$ (***).

3. Results

3.1. Material characterization

By using powder X-ray diffraction (PXRD), the crystalline nature of COF was verified (Fig. 1a). The sharp intense peaks reveals the highly crystalline nature of the compound and peak below 2θ=10° indicates that the material is porous and peaks at 2θ= 5.0°, 6.54°, 7.22°, 12.86°, 14.93°, 16.90°, 18.35°, 19.44°, 22.91°, 23.63°, 24.67°, 26.63°, 28.66° are assigned to 110, 200,011, 002, 101, 111, 102, 013, 122, 113, 130, 123 and 203 reflections respectively. To scrutinise the molecular interaction between synthesized COF with tamoxifen (TMX) and folic acid (FA), Fourier Transform Infrared Spectroscopy (FTIR) was used (Fig. 1c & 1d). For this, the prepared COF and site-targeted tamoxifen-loaded COF were directly measured using FTIR Spectrometer in the scanning range of 4000 to 400 cm^{-1} at room temperature. The FTIR spectrum of the synthesized COF showed a characteristic peak of amide C=O at 1675 cm^{-1} which confirms the formation of COF by amide linkage and other characteristic peaks corresponding to 1245-1323 cm^{-1} is assigned for C-N stretching and peak at 1575 cm^{-1} is assigned for aromatic C=C bending and peaks at 3030 cm^{-1} is assigned to aromatic C-H stretching and the peaks at 3274-3470 cm^{-1} is assigned for N-H stretching vibrations confirms presence of the functional groups and formations of COF[54]. Furthermore, the successful incorporation of the drug molecule, namely tamoxifen, is confirmed by the presence of characteristic peaks of tamoxifen at 1227 cm^{-1} for C-N and peak at 1602 cm^{-1} corresponding to C-O-C present in COF after modification[55,56] and the presence of site targeting agent (folic acid) is also found by the FTIR spectroscopy. Finally, the addition of folic acid to the drug-loaded COF (TMX@COF) was confirmed by the appearance of the C-N stretching group in the region 1015 cm^{-1} and 1279 cm^{-1} [57]. Hence, it is concluded that the successful synthesis of COF and its post-modification with tamoxifen and folic acid was achieved. In addition, a perusal of successful synthesis of COF is confirmed by the solid-state ^{13}C nuclear magnetic resonance (NMR) spectrum. Presence of peak at δ=150 ppm indicates the presence of C=N and peak at δ=65 ppm attributes to C-N and peak between 150-180 ppm corresponds to amide C=O[54], which confirms the formation of COF and is also consistent with the expected structure shown in Fig 1b.

To establish the porosity of COF, Nitrogen adsorption-desorption isotherms at 77 K were done and the Brunauer-Emmett-Teller (BET) surface area was calculated as 28.6494 m^2/g and the pore volume and pore diameter are found to be 0.0269 cc/g and 3.0371 nm, respectively (Fig. S3a). The morphology of synthesized COF is analysed using scanning electron microscopy (SEM) and the images (Fig. 2) show that the COF possess micro flower like porous structure. After drug loading, all the pores were filled with the drug molecule, which is clearly seen in SEM images. Energy-dispersive X-ray spectroscopy (EDX) spectra (Fig. S2) of folate receptor modified tamoxifen loaded COF (TMX@COF-FA) is taken to analyse the elemental compositions. The data revealed that material contains 63.03 % C, 19.62 % N and 17.35 % O.

The thermal stability of the synthesized COF was assessed by thermogravimetric analysis (TGA) and differential scanning calorimetry (DSC). The TGA curve (Fig. S3b & S3c) indicated that the material was thermally stable up to approximately 460 °C. Notably, about 30% of the residue remained undecomposed even upon heating to 700 °C, confirming the high thermal stability of the framework. Furthermore, the chemical stability of the COF was evaluated under harsh acidic and basic conditions by treating it with concentrated sulfuric acid (H_2SO_4) and 5 N sodium hydroxide (NaOH), respectively. The material retained its structural integrity without any observable color change, demonstrating its robust chemical stability. Elemental composition was determined by CHNS analysis. The results confirmed the presence of carbon (65%), nitrogen (11%), and hydrogen (5%) in the COF, which is consistent with its expected chemical structure.

The cytotoxicity of the pristine COF, free tamoxifen (TMX), the non-targeted drug-loaded COF (TMX@COF), and the folic acid-targeted formulation (TMX@COF-FA) was evaluated using the MTT assay (Fig. 3a & b). First, biocompatibility was assessed in L929 fibroblast cells across a concentration range of 10 to 100 µg/mL. The results indicated no significant cytotoxicity in this normal

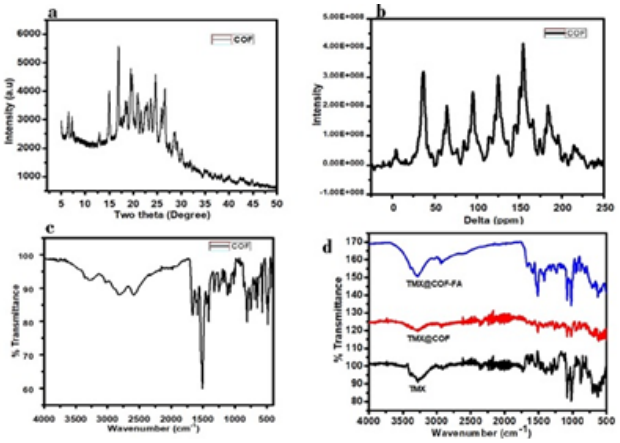


Fig. 1. 1a.) PXRD pattern of the synthesized COF, b) ^{13}C NMR spectra of synthesized COF, c) FTIR spectrum of COF, d) FTIR spectrum of tamoxifen (TMX-Black), TMX@COF (Red), TMX@COF-FA (Blue).

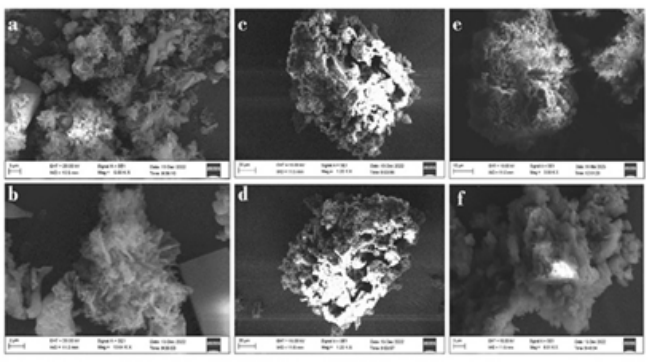


Fig. 2. Scanning Electron Microscopy images of a, b) COF, c, d) TMX@COF, e, f) TMX@COF-FA at different magnifications.

cell line. Subsequently, the anticancer activity of the same formulations was tested against MCF-7 human breast cancer cells at identical concentrations (10–100 µg/mL). As shown in Fig. 3a, the targeted formulation, TMX@COF-FA, exhibited potent and selective cytotoxicity, inducing approximately 92% cell death in MCF-7 cells. This efficacy was significantly greater than that of the non-targeted TMX@COF, free TMX, or the pristine COF alone, highlighting the advantage of the folate-mediated targeting strategy.

The anti-cancer property of the synthesized COF and drug-loaded site-targeted COF was also revealed by live and dead cell staining assays, such as acrydine orange (AO- Green fluorescence) and ethidium bromide (EtBr-reddish orange fluorescence) staining assays[58] (Fig. 4a). The merged images show that there are fewer live cells after incubation with 50 µg/mL of TMX@COF-FA when comparing with COF, TMX@COF and TMX alone. Oxidative stress is a crucial factor for the depletion of tumour cells[59]. A slight increase in reactive oxygen species (ROS) contributes to promoting cell growth, but extremely high ROS levels lead to cellular death[57]. Intracellular ROS generation was measured using the dichloro-dihydro-fluorescein diacetate (DCFH-DA) assay, where fluorescence intensity correlates with ROS levels. Representative fluorescence images (Fig. 4b) revealed a pronounced increase in green fluorescence intensity in MCF-7 cells treated with the targeted formulation, TMX@COF-FA. This intense signal indicates a substantially higher level of ROS induction by TMX@COF-FA compared to cells treated with free tamoxifen (TMX), the non-targeted TMX@COF, or the pristine COF alone. The elevated ROS production is a key mediator of the observed cellular apoptosis.

Flow cytometry (FACS) was employed to quantify the levels of intracellular reactive oxygen species (ROS) in MCF-7 cells, providing a complementary quantitative measure to the imaging data (Fig. S4). Treatment with the various formulations led to a dose-dependent increase in ROS levels. Specifically, the mean fluorescence intensity, representing ROS production, increased to 5.9%, 10.7%, 32.1%, and 52% above the baseline level of untreated control cells following exposure to the pristine COF, free tamoxifen (TMX), the non-targeted TMX@COF, and the targeted TMX@COF-FA, respectively. Notably, cells treated with the targeted formulation (TMX@COF-FA) exhibited a significantly higher ROS level compared to those treated with the non-targeted TMX@COF, free TMX, or the COF alone ($p < 0.001$). These results quantitatively confirm that the potent pro-apoptotic effect of TMX@COF-FA is strongly associated with its ability to induce substantial oxidative stress.

A wound healing (scratch) assay was performed to evaluate the anti-migratory and anti-proliferative potential of the formulations (Fig. S5). Briefly, a confluent monolayer of MCF-7 cells was scratched to create a uniform wound, followed by treatment with the formulations at a concentration of 50 µg/mL. Phase-contrast images of the wound area were captured immediately after scratching (0 h) and at 6-hour intervals over a 24-hour incubation period. The results demonstrated that while untreated control cells exhibited robust migration and wound closure, this process was significantly inhibited in cells treated with the targeted formulation, TMX@COF-FA. The inhibitory effect of TMX@COF-FA on cell migration was markedly greater than that of the non-targeted TMX@COF, free TMX, or the pristine COF. This pronounced anti-migratory activity further substantiates the potent anti-cancer efficacy of the folate-targeted nanocarrier.

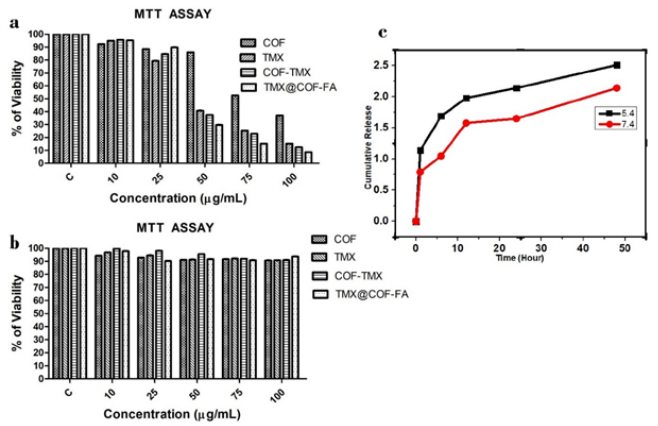


Fig. 3. Cell viability of COF, TMX, TMX@COF, TMX@COF-FA at different concentrations (10, 25, 50, 75, 100 µg/mL) in a) MCF-7 human breast cancer cells, b) in L929 Fibroblast cells, c) Release profile of tamoxifen from TMX@COF-FA at pH 5.4 and pH 7.4.

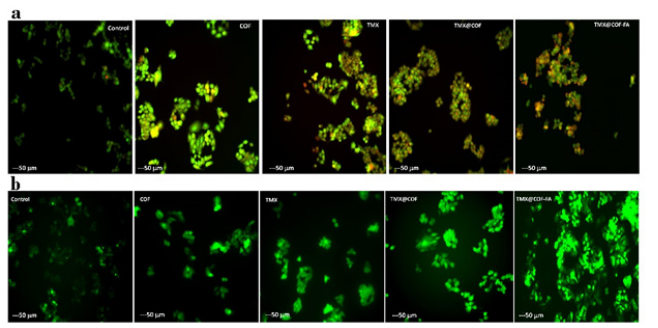


Fig. 4. Fluorescent microscopy images of a) Acrydine Orange, Ethidium Bromide staining of COF, Tamoxifen, TMX@COF, TMX@COF-FA and untreated MCF-7 human breast cancer cells. b) DCFH-DA staining of untreated cells, COF, Tamoxifen, TMX@COF, TMX@COF-FA in MCF-7 human breast cancer cells. Scale bars in fig a & b are 50 µm and the concentration of formulations is 50 µg/mL, number of cells per well is $1x10^4$.

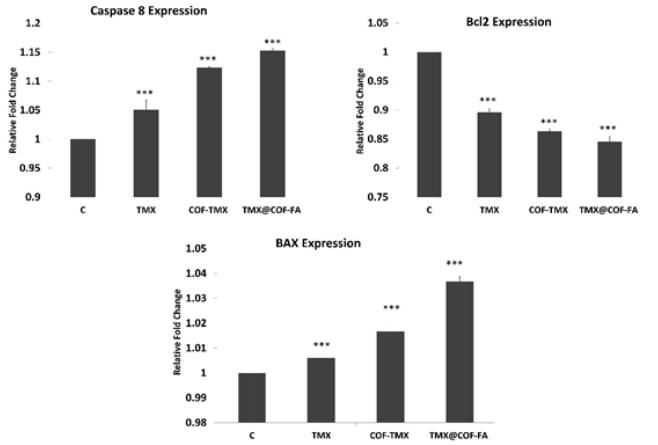


Fig. 5. Gene Expression levels of Control, COF, Tamoxifen, TMX@COF and TMX@COF-FA by q-RTPCR in MCF-7 human breast cancer cells. All the groups are compared control group *, $p \leq 0.05$; **, $p \leq 0.01$; ***, $p \leq 0.001$. The statistical analysis was performed by one-way ANOVA using GraphPad Prism 9.

The drug loading was successfully achieved and analysed by the difference in weight of drug delivery system after loading with tamoxifen and the drug loading efficiency is quantified as 88.5% into the synthesized COF drug delivery system. The release of TMX from the site targeted drug-loaded COF (TMX@COF-FA) was quantified for 48 hours in phosphate-buffered saline at physiological pH (7.4) and pathological (cancerous) pH (5.4). The release of TMX from TMX@COF-FA was found to be high in pathological pH compared to physiological pH after 24 hours (Fig 3c).

4. Discussion

The potential of nanoscale covalent organic frameworks (COFs) in anticancer therapy, particularly for targeted drug delivery, has attracted extensive interest, and their feasibility and efficacy as drug delivery vehicles have been well established [60–62]. The unique characteristics of COFs, such as tunable and permanent porosity, high surface area, ease of surface functionalization, and biocompatibility, make them promising candidates for site-specific drug delivery in cancer therapeutics [39]. To enhance the tumor-specific accumulation of nanocarriers, the surface-targeting ligand folic acid (FA) was employed. In this study, we synthesized a novel COF via a two-step solvothermal method, forming robust amide linkages [44]. The crystallinity of the synthesized COF was confirmed by PXRD analysis, which showed sharp, intense peaks, indicating its highly ordered structure. Additionally, the presence of peaks below $2\theta = 10°$ suggests a porous framework, as a larger d-spacing corresponds to a lower θ value—a finding corroborated by BET surface area analysis, which revealed a pore diameter of 3.0371 nm and a specific surface area of 28.6494 m^2/g [44]. Further characterization by FTIR spectroscopy confirmed the formation of the COF, with a characteristic peak at 1675 cm^{-1} corresponding to the newly formed amide (C=O) bond [54]. Successful drug loading was verified by the appearance of characteristic tamoxifen peaks in the FTIR spectrum [55,56] and by SEM imaging, which showed the initially porous, microflower-like structure to be substantially filled after tamoxifen incorporation. The presence of characteristic folic acid peaks in the FTIR spectrum further confirmed the surface functionalization with FA [57]. The formation of the COF was additionally validated by solid-state ^{13}C NMR spectroscopy [54]. Thermal stability was assessed by TGA, demonstrating that the COF remains stable up to high temperatures. Furthermore, the COF exhibited notable stability in both acidic and basic media, underscoring its robustness for potential biological applications.

A critical attribute of an effective drug delivery vehicle is its capacity for high drug loading. The COF developed in this study demonstrated excellent loading efficiency, encapsulating tamoxifen with a loading capacity of 88.5%. Furthermore, the release profile of tamoxifen from the COF was pH-dependent. Significantly higher cumulative drug release was observed at the acidic pH (5.4) characteristic of the tumor microenvironment compared to physiological pH (7.4). This preferential release under acidic conditions may be attributed to pH-sensitive interactions, such as changes in electrostatic forces between the drug and the carrier matrix, facilitating enhanced drug liberation in pathological settings [47].

An ideal drug delivery system should selectively deliver its payload to target cells while minimizing off-target toxicity [39]. To assess this selectivity, we evaluated the cytotoxicity of the pristine COF, free tamoxifen (TMX), the non-targeted TMX@COF, and the targeted TMX@COF-FA formulation against both L929 fibroblast cells (a normal cell line) and MCF-7 breast cancer cells. The results indicated that all formulations exhibited negligible cytotoxicity toward L929 cells across a concentration range of 10–100 μg/mL. In striking contrast, a dose-dependent cytotoxic effect was observed in MCF-7 cells. The targeted formulation, TMX@COF-FA, demonstrated potent and selective anticancer activity, reducing cell viability to approximately 8% after 24 hours of treatment. This efficacy was significantly greater than that of the non-targeted TMX@COF, free TMX, or the COF alone. The pronounced selectivity and potency of TMX@COF-FA can be attributed to enhanced cellular uptake via folate receptor-mediated endocytosis in the FR-overexpressing MCF-7 cells.

The induction of apoptosis was further analyzed using an acridine orange (AO) and ethidium bromide (EtBr) dual-staining assay. This assay distinguishes live from apoptotic/necrotic cells based on membrane integrity: AO permeates all cells, staining DNA green, while EtBr is excluded by intact plasma membranes and only enters cells with compromised membranes, staining DNA orange-red [58]. Fluorescence microscopy images revealed a markedly higher proportion of orange-red (EtBr-positive) apoptotic cells in populations treated with the targeted formulation, TMX@COF-FA, compared to those treated with free TMX or the non-targeted TMX@COF. In contrast, cultures treated with the pristine COF alone showed a fluorescence profile similar to the untreated control, predominantly composed of viable (green) cells.

Excessively high levels of reactive oxygen species (ROS) are a well-established trigger for apoptotic cell death. While basal ROS production plays a role in cellular signaling, supraphysiological levels cause oxidative damage to lipids, proteins, and DNA. Cancer cells typically exhibit elevated intrinsic ROS generation due to factors such as metabolic hypoxia, oncogene activation, and loss of tumor suppressor function. This altered redox state creates a vulnerability: whereas low-to-moderate ROS levels can promote cancer cell proliferation and survival, exceeding a critical threshold induces lethal oxidative stress and apoptosis [57]. To quantify ROS induction by our formulations, MCF-7 cells were treated with 50 μg/mL of the pristine COF, free TMX, non-targeted TMX@COF, or targeted TMX@COF-FA and analyzed by flow cytometry. The results demonstrated that TMX@COF-FA treatment induced the highest level of ROS, with a mean fluorescence intensity 52% above the untreated control. This significant ROS surge is a key mechanistic driver of the apoptosis observed with TMX@COF-FA, a finding consistent with the qualitative results from the DCFH-DA staining assay.

To delineate the molecular pathway of apoptosis, the effects of free TMX, TMX@COF, and TMX@COF-FA on the mRNA expression of key regulators—BAX, *Bcl-2*, and *Caspase-8*—were analyzed by qRT-PCR. In the intrinsic apoptosis pathway, Bcl-2 functions as a key anti-apoptotic protein, while Bax and Caspase-8 are pro-apoptotic executioners. Consequently, the Bax/Bcl-2 ratio and Caspase-8 activity are critical determinants of cellular

fate, dictating the switch between survival and programmed cell death [58, 63]. The qRT-PCR results revealed that all drug-treated groups exhibited a pro-apoptotic gene expression profile, characterized by the upregulation of BAX and *Caspase-8* and the concurrent downregulation of *Bcl-2*. Notably, this effect was most pronounced in cells treated with the targeted formulation, TMX@COF-FA. The data confirm that TMX@COF-FA most effectively shifts the apoptotic balance by potently suppressing *Bcl-2* while simultaneously activating the expression of BAX and *Caspase-8*, relative to both free TMX and the non-targeted TMX@COF.

Wound healing assay also revealed that the cancer cell migration was completely inhibited by TMX@COF-FA. Among all the formulations, the cell migration was significantly reduced and the wound area remains same after treatment with 50 µg/mL of TMX@COF-FA for 24 hours of incubation. These result supports the anti-cancer property of the formulation by apoptosis in the MCF-7 human breast cancer cells. The cellular apoptosis was also seen from the confocal images (Fig. S3d) of MCF-7 human breast cancer cells before and after treatment with 50 µg/mL of TMX@COF-FA.

In summary, we have successfully fabricated a novel covalent organic framework (COF) and post-modified it with tamoxifen (TMX) and folic acid (FA) to develop a targeted nanotherapeutic system. The successful synthesis and functionalization were confirmed through comprehensive characterization using PXRD, FTIR, SEM, ^{13}C NMR, CHNS, and BET analysis. The constructed system, TMX@COF-FA, demonstrated potent anticancer efficacy via a targeted delivery mechanism. In vitro drug release studies confirmed a pH-responsive profile, with significantly enhanced release under the acidic pathological conditions (pH 5.4) of the tumor microenvironment compared to physiological pH (7.4). Cytotoxicity evaluation revealed the selective action of TMX@COF-FA, which induced significant cell death (~90%) in MCF-7 breast cancer cells while exhibiting minimal toxicity toward L929 fibroblast cells. Apoptosis was further validated by AO/EtBr staining, which showed a markedly higher proportion of dead cells following TMX@COF-FA treatment compared to non-targeted formulations and free drug. Flow cytometric analysis quantified this effect, showing that TMX@COF-FA elevated intracellular ROS levels by approximately 82%, a key driver of the observed apoptosis. qRT-PCR analysis elucidated the molecular mechanism, confirming that TMX@COF-FA effectively upregulated pro-apoptotic genes (BAX, *Caspase*-8) and downregulated the anti-apoptotic gene (*Bcl*-2). Furthermore, a wound healing assay demonstrated the superior anti-migratory and anti-proliferative properties of the targeted formulation. Collectively, these findings robustly indicate that functionalized COFs, particularly our FA-targeted TMX@COF-FA construct, represent a highly promising platform for targeted drug delivery in breast cancer therapy.

Conflicts of interests
The authors have no conflicts with any step of the article preparation.

Consent of publication
The authors read and approved the final manuscript for publication.

Ethics approval and consent to participate
No human or animals were used in the present research.

Informed consent
The authors declare that no patients were used in this study.

Author contributions
Conceptualization: J. P. A. and A.C.; literature collection: A.C and S. S., data curation and original draft writing: A.C., methodology: A.C and S. S.; and reviewing, editing, and finalizing the manuscript: J. P. A., A.C., R.A and M.V. All authors have read and agreed to the published version of the manuscript.

Data Availability
Reasonable requests can be made to the corresponding author to obtain the datasets generated and/or analysed during this research. All relevant data are encompassed in the manuscript and its supplementary information (ESI).

Acknowledgements
The authors gratefully acknowledge financial support from the following funding agencies: the Science and Engineering Research Board (SERB), India (Start-up Research Grant); the University Grants Commission (UGC), India (Start-up Grant for New Faculty); the Government of Kerala; and the University of Kerala (Plan and Non-Plan funds). We also extend our sincere gratitude to the Central Laboratory for Instrumentation and Facilitation (CLIF) at the University of Kerala; Mahatma Gandhi University, Kottayam; Scientium Analyze, Jaipur; and the Rajiv Gandhi Centre for Biotechnology, Thiruvananthapuram, for providing essential instrumentation and technical assistance.

References

1. Akram M, Iqbal M, Daniyal M, Khan AU (2017) Awareness and current knowledge of breast cancer. Biol Res 50, 33. https://doi.org/10.1186/s40659-017-0140-9
2. DeSantis CE, Fedewa SA, Goding Sauer A, Joan L. Kramer, Robert A. Smith, Ahmedin Jemal, et al (2016) Breast cancer statistics, 2015: Convergence of incidence rates between black and white women. CA Cancer J Clin 66:31–42. https://doi.org/10.3322/caac.21320
3. Das SK, Roy S, Das A, Chowdhury A, Chatterjee N, Bhaumik A (2022) A conjugated 2D covalent organic framework as a drug delivery vehicle towards triple negative breast cancer malignancy. Nanoscale Adv 4:2313–2320. https://doi.org/10.1039/d2na00103a
4. Sharath Kumar KS, Girish YR, Ashrafizadeh M, Mirzaei S, Rakesh P K, Zabolian A, et al (2021) AIE-featured tetraphenylethylene nanoarchitectures in biomedical application: Bioimaging, drug delivery and disease treatment. Coord Chem Rev 447:214135. https://doi.org/10.1016/j.ccr.2021.214135
5. Hansen RK, Fuqua SAW (2003) The estrogen receptor and breast cancer. In: Breast Cancer. Humana Press, New Jersey, pp 1–30. https://doi.org/10.1385/0-89603-560-3:1.
6. Sahrayi H, Hosseini E, Karimifard S, Khayam N, Meybodi M S, Amiri S, et al (2021) Co-delivery of letrozole and cyclophosphamide via folic acid-decorated nanoniosomes for breast cancer therapy: Synergic effect, augmentation of cytotoxicity, and apoptosis gene expression. Pharmaceuticals (Basel) 15:6. https://doi.org/10.3390/ph15010006

7. Molani S, Madadi M, Wilkes W (2019) A partially observable Markov chain framework to estimate overdiagnosis risk in breast cancer screening: Incorporating uncertainty in patients adherence behaviors. Omega 89:40–53. https://doi.org/10.1016/j.omega.2018.09.009
8. Madadi M, Molani S, Williams DL (2023) Investigating the effectiveness of supplemental breast cancer screening tests considering radiologists' bias. IISE Trans Healthc Syst Eng 13:1–20. https://doi.org/10.1080/24725579.2022.2095466
9. Fischer HC, Chan WCW (2007) Nanotoxicity: the growing need for in vivo study. Curr Opin Biotechnol 18:565–571. https://doi.org/10.1016/j.copbio.2007.11.008
10. Cho W-S, Cho M, Jeong J, Choi M, Cho Y H, Han S B, et al (2009) Acute toxicity and pharmacokinetics of 13 nm-sized PEG-coated gold nanoparticles. Toxicol Appl Pharmacol 236:16–24. https://doi.org/10.1016/j.taap.2008.12.023
11. Sani A, Cao C, Cui D (2021) Toxicity of gold nanoparticles (AuNPs): A review. Biochem Biophys Rep 26:100991. https://doi.org/10.1016/j.bbrep.2021.100991
12. Prabhu S, Poulose EK (2012) Silver nanoparticles: mechanism of antimicrobial action, synthesis, medical applications, and toxicity effects. Int Nano Lett 2:1 https://doi.org/10.1186/2228-5326-2-32
13. Panyala NR, Peña-Méndez EM, Havel J (2008) Silver or silver nanoparticles: a hazardous threat to the environment and human health? J Appl Biomed 6:117–129. https://doi.org/10.32725/jab.2008.015
14. Zhang X-D, Wu H-Y, Wu D, Wang Y-Y, chang J-H, Zhai Z-B, et al (2010) Toxicologic effects of gold nanoparticles in vivo by different administration routes. Int J Nanomedicine 5:771–781. https://doi.org/10.2147/IJN.S8428
15. Al-Jamal WT, Kostarelos K (2011) Liposomes: From a clinically established drug delivery system to a nanoparticle platform for theranostic nanomedicine. Acc Chem Res 44:1094–1104. https://doi.org/10.1021/ar200105p
16. Bhunia S, Radha V, Chaudhuri A (2017) CDC20siRNA and paclitaxel co-loaded nanometric liposomes of a nipecotic acid-derived cationic amphiphile inhibit xenografted neuroblastoma. Nanoscale 9:1201–1212. https://doi.org/10.1039/c6nr07532k
17. Huang N, Wang P, Jiang D (2016) Covalent organic frameworks: a materials platform for structural and functional designs. Nat Rev Mater 1:10. https://doi.org/10.1038/natrevmats.2016.68
18. Liu Y-J, Cao W-T, Ma M-G, Wan P (2017) Ultrasensitive wearable soft strain sensors of conductive, self-healing, and elastic hydrogels with synergistic "soft and hard" hybrid networks. ACS Appl Mater Interfaces 9:25559–25570. https://doi.org/10.1021/acsami.7b07639
19. Pattni BS, Chupin VV, Torchilin VP (2015) New developments in liposomal drug delivery. Chem Rev 115:10938–10966. https://doi.org/10.1021/acs.chemrev.5b00046
20. Uhrich KE, Cannizzaro SM, Langer RS, Shakesheff KM (2000) Chem Inform Abstract: Polymeric systems for controlled drug release. Chem Inform 31:3. https://doi.org/10.1002/chin.200003275
21. Ding S-Y, Gao J, Wang Q, Zhang Y, Song W-G, Su C-Y, et al (2011) Construction of covalent organic framework for catalysis: Pd/COF-LZU1 in Suzuki-Miyaura coupling reaction. J Am Chem Soc 133:19816–19822. https://doi.org/10.1021/ja206846p
22. Xu H, Gao J, Jiang D (2015) Stable, crystalline, porous, covalent organic frameworks as a platform for chiral organocatalysts. Nat Chem 7:905–912. https://doi.org/10.1038/nchem.2352
23. Wu X, Han X, Xu Q, Liu Y, Yuan C, Yang S, et al (2019) Chiral BINOL-based covalent organic frameworks for enantioselective sensing. J Am Chem Soc 141:7081–7089. https://doi.org/10.1021/jacs.9b02153
24. Peng Y, Huang Y, Zhu Y, Chen B, Wang L, Lai Z, et al (2017) Ultrathin two-dimensional covalent organic framework nanosheets: Preparation and application in highly sensitive and selective DNA detection. J Am Chem Soc 139:8698–8704. https://doi.org/10.1021/jacs.7b04096
25. Huang N, Krishna R, Jiang D (2015) Tailor-made pore surface engineering in covalent organic frameworks: Systematic functionalization for performance screening. J Am Chem Soc 137:7079–7082. https://doi.org/10.1021/jacs.5b04300
26. Zhang G, Li X, Liao Q, Liu Y, Xi K, Huang W, et al (2018) Water-dispersible PEG-curcumin/amine-functionalized covalent organic framework nanocomposites as smart carriers for in vivo drug delivery. Nat Commun 9:2785. https://doi.org/10.1038/s41467-018-04910-5
27. Sun Q, Fu C-W, Aguila B, Perman J, Wang S, Huang H-Y, et al (2018) Pore environment control and enhanced performance of enzymes infiltrated in covalent organic frameworks. J Am Chem Soc 140:984–992. https://doi.org/10.1021/jacs.7b10642
28. Li Y, Chen W, Xing G, Jiang D, Chen L (2020) New synthetic strategies toward covalent organic frameworks. Chem Soc Rev 49:2852–2868. https://doi.org/10.1039/d0cs00199f
29. Tilford RW, Mugavero SJ 3rd, Pellechia PJ, Lavigne JJ (2008) Tailoring microporosity in covalent organic frameworks. Adv Mater 20:2741–2746. https://doi.org/10.1002/adma.200800030
30. Li L, Lu F, Xue R, Ma B, Li Q, Wu N, et al (2019) Ultrastable triazine-based covalent organic framework with an interlayer hydrogen bonding for supercapacitor applications. ACS Appl Mater Interfaces 11:26355–26363. https://doi.org/10.1021/acsami.9b06867
31. Li X, Zhang C, Cai S, Lei X, Altoe V, Hong F, et al (2018) Facile transformation of imine covalent organic frameworks into ultrastable crystalline porous aromatic frameworks. Nat Commun 9:1 https://doi.org/10.1038/s41467-018-05462-4
32. Halder A, Karak S, Addicoat M, Bera S, Chakraborty A, Kunjatt S H, et al (2018) Ultrastable imine-based covalent organic frameworks for sulfuric acid recovery: An effect of interlayer hydrogen bonding. Angew Chem Int Ed 57:5797–5802. https://doi.org/10.1002/anie.201802220
33. Xu H, Tao S, Jiang D (2016) Proton conduction in crystalline and porous covalent organic frameworks. Nat Mater 15:722–726. https://doi.org/10.1038/nmat4611
34. Diercks CS, Yaghi OM (2017) The atom, the molecule, and the covalent organic framework. Science 3;355(6328): eaal1585. https://doi.org/10.1126/science.aal1585
35. Zhang J, Han X, Wu X, Liu Y, Cui Y (2017) Multivariate chiral covalent organic frameworks with controlled crystallinity and stability for asymmetric catalysis. J Am Chem Soc 139:8277–8285. https://doi.org/10.1021/jacs.7b03352
36. Khan N, Slathia G, Kaliya K, Saneja A (2023) Recent progress in covalent organic frameworks for cancer therapy. Drug Discov Today 28:103602. https://doi.org/10.1016/j.drudis.2023.103602
37. Yang S, Liu H (2025) Covalent organic frameworks for immunoassays: A review. Biosensors (Basel) 15:469. https://doi.org/10.3390/bios15070469
38. Li W-Y, Wan J-J, Kan J-L, et al (2023) A biodegradable covalent organic framework for synergistic tumor therapy. Chem Sci 14:1453–1460. https://doi.org/10.1039/d2sc05732h
39. Bhunia S, Deo KA, Gaharwar AK (2020) 2D covalent organic frameworks for biomedical applications. Adv Funct Mater 30:2002046. https://doi.org/10.1002/adfm.202002046
40. Tsoi H, You C-P, Leung M-H, et al (2022) Targeting ribosome biogenesis to combat tamoxifen resistance in ER+ve breast cancer. Cancers (Basel) 14:1251. https://doi.org/10.3390/cancers14051251
41. Early Breast Cancer Trialists' Collaborative Group (EBCTCG),

Davies C, Godwin J, Gray R, Clarke M, Cutter D, et al (2011) Relevance of breast cancer hormone receptors and other factors to the efficacy of adjuvant tamoxifen: patient-level meta-analysis of randomised trials. Lancet 378:771–784. https://doi.org/10.1016/S0140-6736(11)60993-8

42. Cheung A, Bax HJ, Josephs DH, Ilieva MK, Pellizzari G, Opzoomer J, et al (2016) Targeting folate receptor alpha for cancer treatment. Oncotarget 7:52553–52574. https://doi.org/10.18632/oncotarget.9651
43. Fatima M, Sheikh A, Hasan N, Sahebkar A, Riadi Y, Kesharwani P (2022) Folic acid conjugated poly(amidoamine) dendrimer as a smart nanocarriers for tracing, imaging, and treating cancers overexpressing folate receptors. Eur Polym J 170:111156. https://doi.org/10.1016/j.eurpolymj.2022.111156
44. Xu L, Ding S-Y, Liu J, Sun J, Wang W, Zheng QY (2016b) Highly crystalline covalent organic frameworks from flexible building blocks. Chem Commun (Camb) 52:4706–4709. https://doi.org/10.1039/c6cc01171c
45. Devi P, Barry SM, Houlihan KM, Murphy MJ, Turner P, Jensen P, et al (2015) Synthesis and structural characterisation of amides from picolinic acid and pyridine-2,6-dicarboxylic acid. Sci Rep 5:9950. https://doi.org/10.1038/srep09950
46. Rajpoot K, Jain SK (2019) Irinotecan hydrochloride trihydrate loaded folic acid-tailored solid lipid nanoparticles for targeting colorectal cancer: development, characterization, andin vitrocytotoxicity study using HT-29 cells. J Microencapsul 36:659–676. https://doi.org/10.1080/02652048.2019.1665723
47. Matiyani M, Rana A, Pal M, Rana S, Melkani AB, Sahoo NG (2022) Polymer grafted magnetic graphene oxide as a potential nanocarrier for pH-responsive delivery of sparingly soluble quercetin against breast cancer cells. RSC Adv 12:2574–2588. https://doi.org/10.1039/d1ra05382e
48. Abu Lila AS, Soliman MS, Kiran HC, Gangadharappa HV, Younes KM, Khafagy ES, et al (2021) Tamoxifen-loaded functionalized graphene nanoribbons for breast cancer therapy. J Drug Deliv Sci Technol 63:102499. https://doi.org/10.1016/j.jddst.2021.102499
49. Xu L, Li W, Sadeghi-Soureh S, Amirsaadat S, Pourpirali R, Alijani S (2022) Dual drug release mechanisms through mesoporous silica nanoparticle/electrospun nanofiber for enhanced anticancer efficiency of curcumin. J Biomed Mater Res A 110:316–330. https://doi.org/10.1002/jbm.a.37288
50. Mannoush SH, Thaker A A, Jabir M S (2022) Inhibition of Ovarian Cancer Cells Growth Using Gold Nanoparticles and Silica Coated Gold Nanoparticles : In- Vitro Study. J Pham Neg Res 13 (3), 727–733. https://doi.org/10.47750/pnr.2022.13.03.109
51. Lee SY, Kim TH, Choi WG, Chung YH, Ko SG, Cheon C, et al (2023) SH003 causes ER stress-mediated apoptosis of breast cancer cells via intracellular ROS production. Cancer Genomics Proteomics 20:88–116. https://doi.org/10.21873/cgp.20367
52. Chen H, Yu Y, Yang M, Huang H, Ma S, Hu J, et al (2022) YTHDF1 promotes breast cancer progression by facilitating FOXM1 translation in an m6A-dependent manner. Cell Biosci 12:. https://doi.org/10.1186/s13578-022-00759-w
53. Lakshmi S, Renjitha J, B Sasidhar S, Priya S (2021) Epoxyazadiradione induced apoptosis/anoikis in triple-negative breast cancer cells, MDA-MB-231, by modulating diverse cellular effects. J Biochem Mol Toxicol 35:1–17. https://doi.org/10.1002/jbt.22756
54. Wagner-Wysiecka E, Łukasik N, Okuniewski A, Galiński B (2020) Ion recognition properties of new pyridine-2,6-dicarboxamide bearing propeller-like pendant residues: multi-spectroscopic approach. Monatsh Chem 151:331–343. https://doi.org/10.1007/s00706-020-02558-w
55. Maji R, Dey NS, Satapathy BS, Mukherjee B, Mondal S (2014) Preparation and characterization of Tamoxifen citrate loaded nanoparticles for breast cancer therapy. Int J Nanomedicine 9:3107–3118. https://doi.org/10.2147/IJN.S63535
56. Alias D, Yunus R, Chong GH, Che Abdullah CA (2017) Single step encapsulation process of tamoxifen in biodegradable polymer using supercritical anti-solvent (SAS) process. Powder Technol 309:89–94. https://doi.org/10.1016/j.powtec.2016.12.039
57. Rezaei T, Rezaei M, Karimifard S, Beram FM, Dakkali MS, Heydari M, et al (2022) Folic acid-decorated pH-responsive nanoniosomes with enhanced endocytosis for breast cancer therapy: In vitro studies. Front Pharmacol 13:851242. https://doi.org/10.3389/fphar.2022.851242
58. Vikas B, Sujathan K, Rajam SSN, Anil S (2022) Caspase-dependent apoptosis induced by Simarouba glauca on human non-small-cell lung cancer, A549 cells. Asian Pac J Cancer Prev 23:1867–1872. https://doi.org/10.31557/APJCP.2022.23.6.1867
59. Joo JH, Jetten AM (2010) Molecular mechanisms involved in farnesol-induced apoptosis. Cancer Lett 287:123–135. https://doi.org/10.1016/j.canlet.2009.05.015
60. Guan Q, Zhou L-L, Dong Y-B (2022) Construction of nanoscale covalent organic frameworks via photocatalysis-involved cascade reactions for tumor-selective treatment. Adv Ther (Weinh) 5:2100177. https://doi.org/10.1002/adtp.202100177
61. Huo T, Zhang X, Qian M, Nie H, Liang D, Lin C, et al (2022) A space-time conversion vehicle for programmed multi-drugs delivery into pancreatic tumor to overcome matrix and reflux barriers. Adv Sci (Weinh) 9:e2200608. https://doi.org/10.1002/advs.202200608
62. Bhunia S, Saha P, Moitra P, Addicoat MA, Bhattacharya S (2022) Efficacious and sustained release of an anticancer drug mitoxantrone from new covalent organic frameworks using protein corona. Chem Sci 13:7920–7932. https://doi.org/10.1039/d2sc00260d
63. Chen X-X, Leung GP-H, Zhang Z-J, Xiao J-B, Lao L-X, Feng F, et al (2017) Proanthocyanidins from Uncaria rhynchophylla induced apoptosis in MDA-MB-231 breast cancer cells while enhancing cytotoxic effects of 5-fluorouracil. Food Chem Toxicol 107:248–260. https://doi.org/10.1016/j.fct.2017.07.012